

Mechanisms of antibiotic resistance to enrofloxacin in uropathogenic *Escherichia coli* in dog

Cristian Piras^a, Alessio Soggiu^a, Viviana Greco^{b,c}, Piera Anna Martino^a, Federica Del Chierico^d, Lorenza Putignani^e, Andrea Urbani^{b,c}, Jarlath E. Nally^f, Luigi Bonizzi^a, Paola Roncada^{a,g},

^a Dipartimento di Scienze Veterinarie e Sanità Pubblica, Università degli studi di Milano, Milan, Italy

^b Fondazione Santa Lucia – IRCCS, Rome, Italy

^c Dipartimento di Medicina Sperimentale e Chirurgia, Università degli Studi di Roma "Tor Vergata", Italy

^d Metagenomics Unit Bambino Gesù Children's Hospital, IRCCS, Rome, Italy

^e Parasitology and Metagenomics Units, Bambino Gesù Children's Hospital, IRCCS, Rome, Italy

^f Bacterial Diseases of Livestock Research Unit, National Animal Disease Center, Agricultural Research Service, United States Department of Agriculture, Ames, IA 50010, United States

^g Istituto Sperimentale Italiano L. Spallanzani, Milano, Italy

Corresponding author at: Istituto Sperimentale Italiano L. Spallanzani c/o Dipartimento di Scienze Veterinarie e Sanità Pubblica, Università degli Studi di Milano, Via Celoria 10, 20133 Milano. E-mail addresses: paola.roncada@istitutospallanzani.it, paola.roncada@gmail.com, paola.roncada@guest.unimi.it (P. Roncada).

Abstract

Escherichia coli (E. coli) urinary tract infections (UTIs) are becoming a serious problem both for pets and humans (zoonosis) due to the close contact and to the increasing resistance to antibiotics.

This study has been performed in order to unravel the mechanism of induced enrofloxacin resistance in canine E. coli isolates that represent a good tool to study this pathology. The isolated E. coli has been induced with enrofloxacin and studied through 2D DIGE and shotgun MS. Discovered differentially expressed proteins are principally involved in antibiotic resistance and linked to oxidative stress response, to DNA protection and to membrane permeability. Moreover, since enrofloxacin is an inhibitor of DNA gyrase, the overexpression of DNA starvation/stationary phase protection protein (Dsp) could be a central point to discover the mechanism of this clone to counteract the effects of enrofloxacin. In parallel, the dramatic de-crease of the synthesis of the outer membrane protein W, which represents one of the main gates for enrofloxacin entrance, could explain additional mechanism of E. coli defense against this antibiotic. All 2D DIGE and MS data have been deposited into the ProteomeXchange Consortium with identifier PXD002000 and DOI <http://dx.doi.org/10.6019/PXD002000>.

Keywords: *Escherichia coli*, Antibiotic resistance, Urinary tract infections, Enrofloxacin

1. Introduction

Antibiotic resistance in microbes in general and particularly in *Escherichia coli* represents a phenomenon that is dramatically increasing in the last decade. This is due to the use of high amounts of antibiotics in all fields of zootechnical industry [1–5].

E. coli also represents a serious burden for human health because of its spread in the environment. It could be found in skin, in surgical infections and in several other types of epithelial tissues. Because of its high presence in the environment, its infection could be quite common and antibiotic resistance actually represents a serious problem especially in the light of last experimental evidences that document how E. coli is developing high rates of multidrug resistance [6].

One of the most frequent infections of this pathogen for humans is caused by extra-intestinal pathogenic E. coli (ExPEC). It can colonize urinary tract causing urinary tract infections (UTIs). In worst cases, septicemia and meningitis can occur [7]. It has been estimated that about 50% of all women can suffer from UTI at least one time in their life [8] and that in most cases it could be recurrent. The analysis of the genome of several E. coli isolates demonstrated the direct link between production animals, meat and human UTI giving the basis to consider UTI as a real zoonosis [9]. The mechanisms behind the consumption of food from animal production and UTI are still unknown, however, there are evidences that document how resistant E. coli can jump from food to human extraintestinal pathogenic E. coli [10]. The similarity between UTI animal infections and human was documented by Johnson and colleagues who also proposed the dog as animal model and natural reservoir [11,12]. In this article, the role of dog as reservoir of "human" uropathogenic E. coli for acquisition by susceptible human hosts is well described [11,13,14]. According to the described experimental evidences it is possible to hypothesize the jump of mutated or resistant strains of E. coli from dog to humans. The antibiotic resistance of E. coli isolates from dogs has been as well already documented [15] and in particular to enrofloxacin that actually represents one of the most used antibiotics to counteract this infection [16]. Fluoroquinolones are inhibitors of bacterial DNA replication through the block of topoisomerase and DNA gyrase [17]. Thus, this results in DNA supercoiling and in related DNA damage [18]. The genetic mechanism of E. coli resistance to fluoroquinolone action has already been documented [19]. Different experiments show how the development of antibiotic resistance could be due to mutations of the genes encoding DNA gyrase and topoisomerase IV [20]. However, this adaptation is not the only one responsible for the development of E. coli fluoroquinolone resistance, that depends not directly from genome mutations but for example from the loss of membrane porins or the augmented drug extrusion through the efflux pumps [20].

Apart from these evidences, the cellular response and the adaptive mechanisms developed by E. coli to counteract the action of this drug still have to be elucidated through the analysis of the differential proteome. In the last decades, the study of proteome in antibiotic resistance provided a valid contribution to a better understanding of the mechanisms of this phenomenon. Therefore, the aim of this study was to perform a deeper investigation of possible molecular pathways involved in the antibiotic resistance.

The differential proteomic profiling between sensitive and enrofloxacin-resistant (induced) E. coli isolates from UTIs of dogs has been evaluated. The E. coli isolate was treated with growing concentration of enrofloxacin up to 10 µg/ml. Both sensitive and exposed isolates were discriminated through the biochemical and antibiotic resistance profiles and the proteomic analysis has been performed by two complementary methodologies based on 2D DIGE and shotgun MS analysis. These approaches led us to highlight some proteins differentially expressed that could play a key role in antibiotic resistance and could become possible targets to counteract multidrug resistance.

2. Methods

2.1. Bacterial isolation and characterization

2.1.1. Bacterial culture

E. coli strain was chosen among the collection of canine isolates from urine of dogs affected by cystitis. Briefly, 200 μ l of urine sample was streaked onto blood agar plates (Oxoid, Italy) and incubated at 37 °C for 18–24 h under aerobic condition.

Bacterial identification was performed by evaluating the colony morphology, using Gram staining and biochemical tests; also API 20E (BioMérieux, France) was used to identify *E. coli* strain more accurately.

For induction of antibiotic resistance, bacterial cells of this isolate were cultured in Mueller-Hinton broth (Oxoid, Italy) with increasing enrofloxacin concentration of up to 10 μ g/ml. Three biological replicates of this isolate before enrofloxacin induction were grown in Mueller-Hinton broth (Oxoid, Italy) without antibiotic (sensible isolate) in order to have the control group (C). Three biological replicates were grown with 10 μ g/ml of enrofloxacin (after resistance induction) in order to have the stable resistant group (E). The Kirby–Bauer test was used to confirm the sensitivity to enrofloxacin of isolated strain. Once the bacterial concentration of 10^{10} UFC/ml ($n^{\circ}5$ McFarland standard; BioMérieux, France) was reached in each culture, cells were harvested through centrifugation at 3000 g for 15 min at 4 °C. Cell pellet was washed 6 times in PBS and stored at –20 °C up to protein extraction procedure.

2.2. Vitek-2 ID and susceptibility test

Identification and antimicrobial susceptibility tests were performed by using Vitek 2.0 system with VITEK 2 GN and AST-N201 cards, for antimicrobial susceptibility testing, respectively, according to the manufacturer's instructions (BioMerieux, Marcy l'Etoile, France). As reference strain, *E. coli* ATCC 25922 was used (http://www.lgcstandards-atcc.org/products/all/25922.aspx?geo_country=it).

2.3. MALDI-TOF biotyper

E. coli cells from single colonies were carefully scraped and washed in H₂O/CH₃CH₂OH (1:3 v/v) and further treated for MALDI-TOF MS fingerprinting profile according to Putignani et al. [21]. The dry pellets were mixed thoroughly with 70% formic acid (HCOOH) and ACN (50 μ l/ each) (Sigma-Aldrich, Milan, Italy). 1 μ l of the protein mixture was mixed with an isovolume of CHCA matrix in 50% ACN/2.5% TFA (1.5 μ l) (Sigma-Aldrich) and placed onto an MSP 96 polished steel target (Bruker Daltonics GmbH, Bremen, Germany) [21]. Protein mass spectra were acquired using a Microflex MALDI-TOF-MS (Bruker Daltonik GmbH) mass spectrometer in linear positive mode at maximum frequency (20 Hz). Measured spectra mass range was from 2000 to 20,000 Da, according to manufacturer's protocol. Spectral measurements were performed with a Microflex LT mass spectrometer (Bruker Daltonics), using FlexControl software (version 3.0, Bruker Daltonics). Eight technical replicates for each spectrum were collected for each species and analyzed for reproducibility, 500 laser shots/spot were manually collected, employing the FlexControl software package. Spectra profiles were visualized by FlexAnalysis 3.0 software Bruker Daltonics. Pearson's correlation coefficient was calculated from the spectra row data by R-bioconductor to establish the intra (replicates) and interstrain condition reproducibility (ranging from 0.89 to 0.98).

2.4. Proteomics analysis

2.4.1. Protein extraction

About 50 mg of cellular pellet for each sample was collected. Cell pellets were washed three times in a cold washing solution containing 10 mM tris and 1 mM EDTA and then collected by centrifugation at 1500 g for 5 min at 4°. 300 μ l of buffer solution (7 M urea, 2 M thiourea, 1% ASB-14) was added to each sample and solubilized by pipetting. Protein concentration was measured using Biorad Protein Assay kit following manufacturer instructions.

2.4.2. 2D DIGE

All samples were adjusted to a protein concentration of 5 μ g/ μ l and adjusted to pH 8.6. 2D DIGE kit (Amersham CyDye DIGE Fluor Kits, product code 25-8010-65) was used according to the manufacturer instructions. The labeling of the dyes was performed as described in Table 1 of Supplementary material.

150 μ g of labeled proteins was loaded on a 24 cm 4–7 Ipg strip rehydrated overnight with a final volume of 450 μ l of rehydration buffer (7 M urea, 2 M thiourea, 1% ASB-14, 30 mM DTT, 0.5% IPG buffer, 0.01% bromophenol blue) in dark. The isoelectric focusing was carried out in an IPG-Phor apparatus (GE) up to 80,000 Vhr at a maximum voltage of 8000 V. After the first dimension, the strips were equilibrated in a buffer containing 6 M urea, 2% SDS, 0.05 M Tris, 20% glycerol, and 1% DTT for 15 min and afterwards in the same buffer except with 2.5% iodoacetamide instead than DTT for another 15 min. The second dimension (Ettan DALTsix electrophoresis unit) was carried out in 12% acrylamide gel at a constant power of 1 W per gel.

2.4.3. Image analysis and statistical analysis

After the second dimension, gels were not removed from the plates, washed in distilled water and covered in tinfoil to preserve the dyes. Image acquisition was performed with a Typhoon apparatus (GE) following manufacturer protocol. Briefly, the first scan of each gel of each dye was performed at 500 μ m in order to set the DMT value to achieve a similar target value between 50,000 and 80,000 and within 15,000 from each other. The final scan for each dye was performed at 100 μ m. Image files in gel format were analyzed through 2D DIGE module of SameSpots software (Version 4.5, Nonlinear Dynamics U.K.). Spots with a p value lower than 0.05 and a fold change higher than 2 were taken into consideration for further mass spectrometry analysis and protein identification.

Micropreparative 2D electrophoresis for spot cutting was carried out loading 600 μ g of protein sample in a 24 cm, pH 4–7 IPG strip (focusing protocol: passive rehydration, 100 V/6 h, 300 V/4 h, 8000 V/6 h, 8000 V/90,000 VhT). The second dimension was carried out as for the DIGE procedure. The matching was also done with SameSpots software and spots were manually excised.

2.4.4. Protein identification from two-dimensional electrophoresis gel

The protein identification was performed according to the methodological protocol previously described [6,22–24]. Briefly, after steps of dehydration, reduction and alkylation, single spots were digested with a solution of 0.01 μ g/ μ l of porcine trypsin (Promega, Madison, WI) at 37 °C for 16 h. Peptides were concentrated using C18 ZipTip (Millipore) and then were spotted on a Ground Steel plate (Bruker-Daltonics, Bremen, Germany).

The MS analysis was performed on a Ultraflex III MALDI-TOF/TOF spectrometer (Bruker-Daltonics) in positive reflectron mode. For the external calibration, the standard peptide mixture calibration (Bruker-Daltonics: m/z: 1046.5418, 1296.6848, 1347.7354, 1619.8223, 2093.0862, 2465.1983, 3147.4710) was used. To select monoisotopic peptide masses, mass spectra were analyzed with FlexAnalysis 3.3 software (Bruker-Daltonics). After an internal calibration (known autolysis peaks of trypsin, m/z: 842.509 and 2211.104) and exclusion of contaminant ions (known matrix and human keratin peaks), the created peak lists were analyzed by MASCOT v.2.4.1 algorithm (www.matrixscience.com) against SwissProt 2014_10 database restricted to *E. coli* taxonomy (22993

sequences). For database search these parameters were established: carbamidomethylation of cysteines and oxidation on methionines were set respectively among fixed and variable modifications, one missed cleavage site was set for trypsin and maximal tolerance was established at 70 ppm. For protein identification assignment only Mascot scores higher than 56 were considered significant ($p < 0.05$). To confirm the identification obtained, MS/MS spectra were acquired by switching the instrument in LIFT mode with $4-8 \times 10^3$ laser shots using the instrument calibration file. For the fragmentation, precursor ions were manually selected and the precursor mass window was automatically set. For each MS/MS spectra acquired, spectra baseline subtraction, smoothing (Savitsky–Golay) and centroiding were operated using Flex-Analysis 3.3 software. These parameters have been used for database search: among fixed and variable modifications, carbamidomethylation of cysteines and oxidation on methionine were set respectively, maximum of one missed cleavage was established, the mass tolerance was set to 50 ppm for precursor ions and to a maximum of 0.5 Da for fragments. The taxonomy was restricted to *E. coli* (22993 sequences). The confidence interval for protein identification was set to 95% ($p < 0.05$) and only peptides with an individual ion score above the identity threshold were considered correctly identified.

2.4.5. Expression analysis by nLC–MS^E

Shotgun analysis was performed as previously described in [25,26]. Briefly, protein extracts of six samples were precipitated with a cold mix of ethanol, methanol, and acetone (ratio 2:1:1, v/v), then dissolved in 6 M urea and 100 mM Tris at pH 7.5, and digested 50:1 (w/w) with sequence grade trypsin (Promega, Madison, WI, USA) at 37 °C overnight after reduction with 10 mM DTT and alkylation with 20 mM IAA. The reaction was stopped by adding a final concentration of 0.1% TFA. Separation of tryptic peptides and subsequent qualitative and quantitative nLC–MS^E analysis were performed by nanoACQUITY UPLC System (Waters Corp., Milford, MA) coupled to a Q-ToF Premier mass spectrometer (Waters Corp., Manchester, U.K.). An amount of 100 fmol/μl of digestion of Enolase from *Saccharomyces cerevisiae* was added to each sample as internal standard, then a final concentration of 0.6 μg of protein digestion was loaded on column for peptide separation. Peptides were loaded onto a Symmetry C18 5 μm, 180 μm × 20 mm precolumn (Waters Corp.) and subsequently separated by a 170 min reversed phase gradient at 250 nL/min (3–40% CH₃CN over 145 min) using a NanoEase BEH C18 1.7 μm, 75 μm × 25 cm nanoscale LC column (Waters Corp.) maintained at 35 °C. The Q-ToF Premier mass spectrometer directly coupled to the chromatographic system operated in “Expression Mode” switching between low (4 eV) and high (15–40 eV) collision energies on the gas cell, using a scan time of 1.5 s per function over 50–1990 m/z. The processing of low and elevated energy, added to the data of the reference lock mass, provides a time-aligned inventory of accurate mass-retention time components for both the low and elevated-energy (EMRT, exact mass retention time).

Each sample was run in four technical replicates. For qualitative and quantitative analysis, LC–MS data from four replicate experiments for each six samples were processed using ProteinLynx GlobalServer v.3.0.2 (PLGS, Waters Corporation). Protein identifications were obtained with the embedded ion accounting algorithm of the software searching into UniProtKB/Swiss-Prot *E. coli* database release 2013_12 (25 245 entries) to which the sequence of enolase (UniProtKB/Swiss-Prot AC: P00924) was appended. These search parameters were set: automatic tolerance for precursor ions and for product ions, minimum 3 fragment ions matched per peptide, minimum 7 fragment ions matched per protein, minimum 2 peptide matched per protein, 1 missed cleavage, carbamidomethylation of cysteines and oxidation of methionines as fixed and variable modifications, false positive rate (FPR) of the identification algorithm under 1% and 100 fmol of the enolase internal standard set as calibration protein concentration. The most reproducible proteotypic peptides for retention time and intensity of enolase digestion (m/z 745.43; m/z 814.49; m/z 1288.70; m/z 1416.72; m/z 1578.80, m/z 1840.89) were used to normalize the EMRTs table. The expression analysis was performed considering 12 technical replicates available for each experimental condition (i.e., one experimental condition, control and enrofloxacin resistant group, × three biological replicates × four technical replicates) following the hypothesis that each group is an independent variable. The protein identifications were based on the detection of more than two fragment ions per peptide, more than two peptides measured per protein. The list of normalized proteins was screened according to the following criteria: protein identified in at least 3 out of 4 runs of the same sample with a fold change of regulation higher than ± 20%; only modulated proteins with a $p < 0.05$ were considered significant. The protein quantification was performed adding to each sample as internal standard digestion of enolase from *S. cerevisiae* according to Silva JC et al. [27,28].

The mass spectrometry proteomics data have been deposited to the ProteomeXchange Consortium [29,30] via the PRIDE partner repository with the dataset identifier PXD002000 and DOI <http://dx.doi.org/10.6019/PXD002000>.

2.4.6. Bioinformatic data analysis

2.4.6.1. Protein functional signatures by InterProScan and MEGAN, *E. coli*

Uniprot accession numbers were converted in a unique fasta file using the Uniprot Retrieve/ID Mapping tool. Fasta sequences for each protein were functionally classified using the local version of the InterProScan 5 tool [31]. GO terms were retrieved using the `–goterm iprscan` option. PANTHER (Protein ANalysis THrough Evolutionary Relationships) classification [32] was obtained using the `–appl iprscan` option.

An explorative analysis to check the KEGG/SEED functional profiles associated to each group was performed with MEGAN software. Briefly, ProteinLynx GlobalServer (PLGS) v3.0.2 *.csv files containing all the identified peptides obtained from the processed spectra were filtered using a Python script to extract only all the non-redundant peptide sequence information and converted in a fasta file. The sequence similarity search was done using the BLAST+ program (version 2.2.30) [33]. The blastp-short application optimized for short query sequences was used to check the sequences against a non-redundant protein sequences database (<ftp://ftp.ncbi.nih.gov/blast/db> nr.*tar.gz 27.01.2015) limited to the *E. coli* taxon. We set a lower E-value (10^{-5}) to achieve a good stringency to obtain very close matches to the protein database and to reduce the number of false positives. Output files from BLAST+ were imported on the MEGAN software (version 5.7.2) [34] to obtain the functional analysis using the SEED/KEGG classification function. The LCA algorithm parameters were set as following to keep a high quality matches: (min support 5, min score 35, max expected 10^{-5} , top percent 10).

3. Results

Proteins represent the main contributors to the mechanisms involved in antibiotic resistance in bacteria. Their abundance profile provides reliable information about the mechanisms involved in this process. Three biological replicates of control and resistant groups have been analyzed both through 2D DIGE and shotgun proteomics. The whole dataset is described below.

3.1. Biochemical classification and antibiotic resistance profile

The resistance to enrofloxacin was induced through increasing concentrations of enrofloxacin in order to evaluate the adaptive response. All experimental groups were found to be positive to indole test and to motility test.

Once the isolate was induced to grow in presence of enrofloxacin up to a concentration of 10 µg/ml, both the biochemical characterization and the antibiotic resistance profile among experimental groups were performed.

The identification of the strain (*E. coli* isolate sensible and resistant to enrofloxacin and a reference strain ATCC 25922) was performed by the Vitek-2 system, based on biochemical profile. Both isolate and reference strains were identified as *E. coli* with excellent reliability (Table 2, supplementary material). Both sensitive and resistant isolates showed the same exact biochemical profile that was different from the ATCC 25922 profile. The antimicrobial analyses showed a similar resistance pattern in resistance and sensitive isolate. In particular, they were resistant to amoxicillin/clavulanic, piperacillin/tazobactam, cefotaxime, cefepime molecules, and sensitive to the remaining tested drugs, while *E. coli* ATCC 25922 strain resulted sensitive to all tested antimicrobial molecules (Table 3, supplementary material). This result demonstrates the different biochemical and antimicrobial profile between isolated and ATCC 25922 strains. Moreover, it was interesting to note how the resistance profile was the same between control and sensitive isolate highlighting that, with the exception of enrofloxacin, the profile of all other antibiotics was invariated (Table 3, supplementary material).

MALDI-TOF MS Biotyper was used to obtain the fingerprinting peptide profile of the analyzed isolates (Fig. 1, Panel A).

Dendrograms derived from MALDI-TOF MS Biotyper profiles showed a cluster formation due to differences on proteic patterns of the strains under study. In particular, the spectra dendrogram showed two main clusters (Fig. 1, Panel B). The first cluster grouped the 8 sample replicae belonging to enrofloxacin resistant *E. coli*, the second one is composed by two distinct sub-clusters belonging to sensitive *E. coli*. PCA analysis showed that, along PC1, replicae from resistant *E. coli* were well separated from sensitive isolate, that grouped together with reference strain (Fig. 1, Panel C).

3.2. 2D DIGE and protein identification

Results highlighted 19 differentially expressed proteins (Table 1). All the differentially expressed proteins detected using the Progenesis SameSpots software were filtered according to a p-value ≤ 0.05 and to a fold change ≥ 2 . In Fig. 3 it is possible to see a general scheme representing the differential expression of each protein with the details obtained from the 2D DIGE experiment.

Spots of interest were manually excised, trypsin digested and analyzed by peptide mass fingerprinting (PMF) and MS/MS. Using the Swiss Prot database restricted to *E. coli*, only one protein has been identified for each spot.

In Fig. 4 it has been represented an output of the classification of the identified proteins through Panther according to GO Molecular function classification of the identified proteins.

Table 1 provides the list of identified proteins through 2DE. Proteins have been grouped according to their function that include (metabolism, oxidative stress, membrane transport, cell-cell communication, DNA-repair, other metabolism) and all the mass spectrometry data.

3.3. Shotgun proteome profiling by label-free nUPLC-MS^E

A comparative proteome analysis between two groups, control group (C) and enrofloxacin resistant (E), based on nLC-MS^E, has been performed. A total of 86841 EMRTs and 670 proteins were qualitatively identified across both conditions. Quantitative analysis was performed after EMRTs and protein normalization. Applying this experimental approach, a total of 57 differentially expressed proteins were highlighted. These included the 19 proteins already highlighted in 2D analysis and other 38 differentially expressed (Table 2). Interestingly it is possible to observe a congruency in expression trends between 2D-DIGE comparative analysis and results obtained by label-free differential analysis. In fact, all of the spots showed similar trends in expression change by both proteomic approaches (Table 1). This result represents a validation of data obtained via 2DE and confirms the reliability of obtained data.

3.4. Functional features of identified *E. coli* proteins

Briefly, for GO analysis, all accession numbers of differentially expressed proteins (up and down regulated) have been analyzed in order to highlight the mechanisms involved in the different strains. Obtained results are shown in Fig. 3.

To better investigate the functional differences belonging to the two groups of *E. coli*, the entire dataset of all peptides identified via shotgun MS was analyzed using the Interproscan 5 tool and the MEGAN software. Fig. 5 resumes the obtained results representing the most important proteins according to function, location and expression among groups. This approach allowed the comfortable visualization of the roles of differentially expressed proteins in the regulation of the bacterial pathways.

4. Discussion

In the present study, a comparative proteomic investigation was performed to identify proteins associated with resistance to enrofloxacin in *E. coli*, allowing us to get deeper insights in the complex mechanism of acquired resistance to this antibiotic.

Biochemical and antibiotic resistance profiling were performed in order to give more completeness to this study. Data showed in Tables 2 and 3 of supplementary material highlighted that both control and resistant bacteria had exactly the same biochemical and antibiotic resistance profile that was different from the reference strain. This result confirms that not biochemical, nor antibiotic resistance pattern has changed in the strain that became resistant, but only sensitivity to enrofloxacin.

On the contrary, MALDI TOF MS-based fingerprinting results (Fig. 1), highlighted that the protein expression pattern was different among reference ATCC 25922, sensitive and resistant *E. coli* isolates.

Molecular fingerprint represents the first step for the characterization of phenotypic differences among bacteria. The successful application of MS profiling of intact microbes for their characterization has been well documented [35,36]. It has also been documented how this technique is able to provide interesting information about antibiotic resistance with the advantage of limited costs and time consumption [37]. In our case, prior to perform the proteomics analysis, the screening with MS profiling of control and resistant isolates was performed highlighting the differences among strains and successfully clustering experimental strains according to PC analysis (PCA). The Fig. 1 highlights the diagram obtained after PCA, besides the analysis of the control and resistant isolate it was also included the analysis of a reference ATCC 25922 *E. coli* strain. The results clearly demonstrate differential profiles in peptide protein expression among clusters and between isolate and reference strain. This preliminary result was necessary to decide whether proceed with further experiments such as 2D DIGE and shotgun MS.

According to these preliminary results, the protein profile of the re-sistant group was compared with the one of its sensitive counterpart by a proteomic analysis based on 2D-DIGE to separate proteins combined to MALDI MS analysis and database search to identify differentially expressed proteins. This analysis showed the modulation of 19 proteins between the two conditions. At the same time, another comparative proteomics investigation was also carried out by free-label nLC-MS^E. This method has allowed the qualitative and quantitative analysis of total protein extracts of the two groups for the simultaneous screening of a larger number of proteins. Based on the results a total of 57 differentially expressed proteins were identified and a comprehensive study on the proteins associated with enrofloxacin resistance was carried out. We classified these modulated proteins by their molecular functions and pathways where they are principally involved.

4.1. Metabolism

According to obtained data, energetic metabolism of *E. coli* resistant is generally depressed. This is logic because during the 'status' of antibiotic resistance bacteria try to survive and earn energy to fight against the anti-biotics. The following proteins have been found to be differentially expressed.

4.1.1. ATP synthase subunit b (P0ABA0)

The link between defective ATP synthase and antibiotic resistance has been already described. In 1989 Humbert and Altendorf described a strain of *E. coli* cross-resistant to gentamicin, neomycin and streptomycin that was found to be defective for gamma subunit of ATP synthase (F1F0) [38]. A different result was found in *S. enterica* after quinolones exposure. ATP synthase, subunit b, was found to be increased after ciprofloxacin exposure [39]. As showed in Figs. 2, 3 and Table 1, obtained results highlighted a significantly decreased expression of ATP synthase, subunit b. This result may reflect the adaptive mechanism of the cell in the way of a silent mode in order to reduce the production of more oxidative stress. At the same time the *E. coli* cells are increasing the energy production from glycolysis. Another reason for the decreased expression of ATP synthase could be due to the different use of reducing power: in normal conditions reducing power can be used to generate the H⁺ gradient among the membrane in order to produce ATP, but, under oxidative stress conditions, such as enrofloxacin exposure, the reducing power is necessary to avoid oxidative-stress dependent DNA damage. As shown in Fig. 5, bioinformatic data analysis of obtained shotgun profiles confirmed the described evidence highlighting a decreasing amount of the bacterial subunits of ATP synthase.

4.1.2. Glucokinase (P0A6V8)

This is the first enzyme of glycolysis and is strongly down-regulated according to many of the enzymes of carbohydrate metabolism.

Shotgun MS analysis (Table 2) confirmed as well the previously described findings highlighting the down-regulation in the resistant group of proteins such as citrate synthase, succinate dehydrogenase, malate dehydrogenase and phosphoenolpyruvate synthase. This suggests that cells growing under enrofloxacin concentration present a decreased metabolism (Fig. 5).

4.1.3. Alpha galactosidase (P06720)

The down-regulation of α -galactosidase in resistant group is a new finding that emerged from obtained results. This result was firstly observed through 2D DIGE and successively confirmed by shotgun MS analysis (Fig. 3, Table 1) that also highlighted a strong down-regulation in resistant isolates.

4.1.4. Glucose-specific phosphotransferase enzyme IIA component (P69783)

This protein is also involved in carbohydrates and sugar metabolism and is increased in resistant isolate as highlighted both by 2D DIGE experiments and shotgun MS analysis. It is part of the major carbohydrate transporter system and catalyzes the phosphorylation of incoming sugar substrates concomitantly with their translocation across the cell membrane. One of the GO terms (GO:0045912) associated with this protein is closely related to the negative regulation of carbohydrate metabolic process. Its up-regulation is in agreement with increased metabolism of carbohydrates in the resistant isolates in comparison with the control isolates.

Fig. 1. MALDI-TOF MS based fingerprinting profile of *E. coli* resistant (E), sensitive (C) and ATCC 25922 reference (R) strains. Panel A. Spectral patterns. Panel B. Spectra dendrogram obtained by principal component dendrogram (PCA) analyses for 8 replicae of each strains (resistant, sensitive and ATCC 25922 that is sensitive as well). Panel C. PCA analysis (8 replicates each strains).

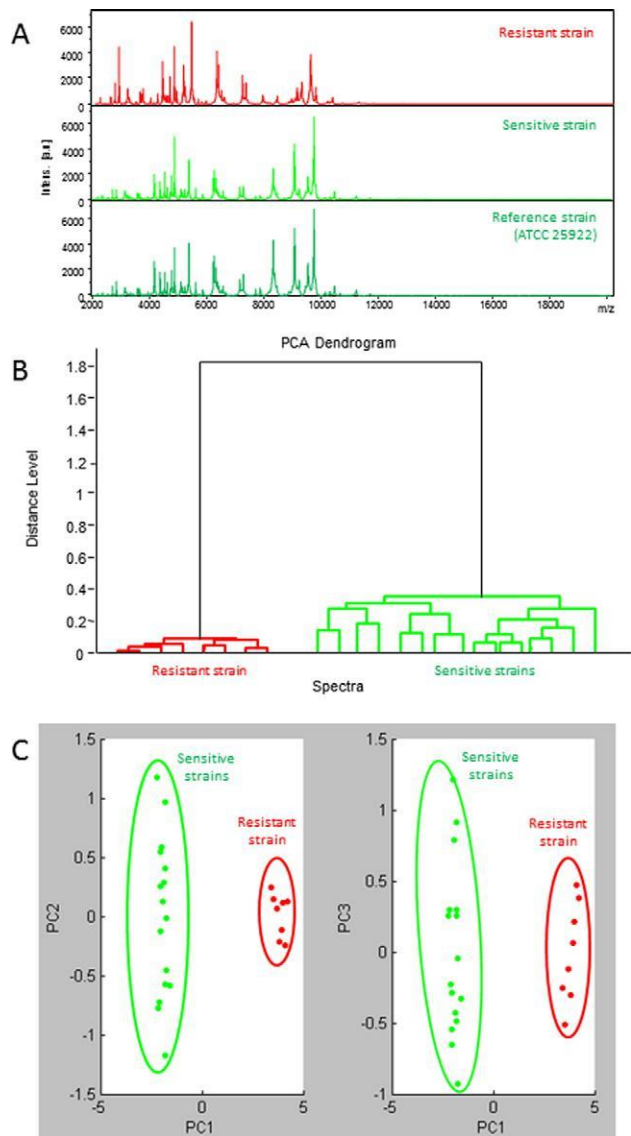


Table 1

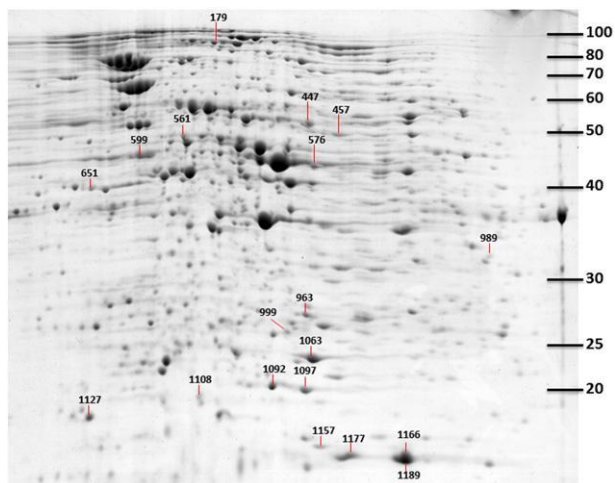
Resume of the proteins differentially expressed identified through 2D DIGE and MALDI TOF MS. The expression values obtained through shotgun MS analysis and the protein quantifications are reported in the last three columns.

Pathway	Spot number	Accession	Description	Mass (Da)	Regulation (R vs C) trend/fold change/p value	Highly represented	Protein Concentration (fmol) R: C	p-Value (t-test)
Metabolism	447	P06720	Alpha galactosidase	51323	↓3.1/0.00227	C	n.q/9.10	b0.0001
	1157	P0ABA0	ATP synthase subunit b	17310	↓2.2/0.0307	C	n.q/3.31	b0.0001
	989	P0A6V8	Glucokinase	35043	↓3.8/0.00119	C	n.q/4.94	b0.0001
Oxidative stress	561	P00350	6 phosphogluconate dehydrogenase decarboxylating	51548	↑2.1/0.00101	R	5.99/2.64	0.0001
	1063	P28304	Quinone oxidoreductase 1	20901	↑3.3/0.00124	R	12.39/n.q	b0.0001
	1097	P0AGD3	Superoxide dismutase [Fe]	21179	↑2.9/0.00493	R	4.63/n.q	b0.0001
	651	P14375	Transcriptional regulatory protein ZraR	36521	↑2.1/0.0397	R		
Membrane transport	1092	P0A915	Outer membrane protein W	21661	↓2.9/0.0219	C	n.q/26.09	b0.0001
	1127	P69783	Glucose-specific Phosphotransferase enzyme IIA component	17870	↑2.5/0.0492	R		
	457	P0A853	Tryptophanase	51820	↓3.9/0.0014	C	n.q/15.07	b0.0001
Cell-cell communication and quorum sensing	576	Q46803	Aspartate/ornithine carbamoyltransferase protein	44497	↓3/0.0498	C	n.q/4.92	b0.0001
	963	P12758	Uridine phosphorylase	27991	↑2.9/0.0165	R	3.16/1.25	0.0001
DNA repair	1177	P0ABT2	DNA protection during starvation protein dps	18684	↑4.4/0.00186			
	1166	P0ABT2	DNA protection during starvation protein dps	18684	↑4.2/0.00214	R	128.36/43.25	0.0001
	1189	P0ABT2	DNA protection during starvation protein dps	18684	↑2.1/0.0143			
	999	P77170	Putative DNA-invertase from lambdoid prophage Qin	28143	↓2.4/0.00244	C		
Other metabolisms	179	P28629	Biodegradative arginine decarboxylase	84982	↑2/0.00555	R	8.35/n.q	b0.0001
	599	P23845	Sulfate adenyltransferase subunit 1	45288	↓2.6/0.031	C	n.q/3.22	b0.0001
	1108	P0AES2	Glucarate dehydratase	18765	↑4.6/0.00307	R		

In this column the arrows represent the trend of expression of each protein (resistant R vs control isolate C), the second number is the fold change according to 2D DIGE profile and the third number is the significance.

In this column, the term nq means below instrumental detection limit.

Fig. 2. Image of micropreparative 2D electrophoresis showing the position of the proteins excised for MALDI TOF analysis.



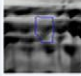
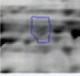
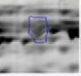

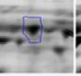
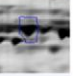
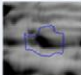
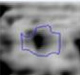
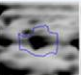
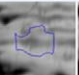
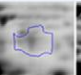
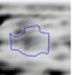
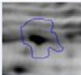
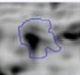
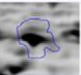
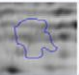
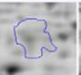
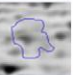
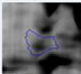
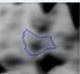
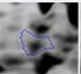
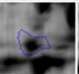
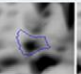
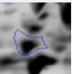
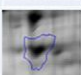
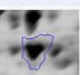
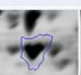
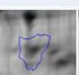














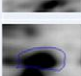

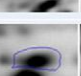



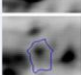
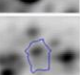
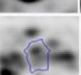
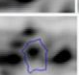
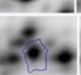
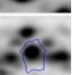
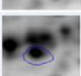
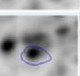
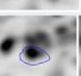
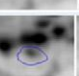
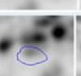
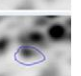
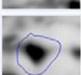
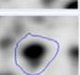
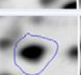
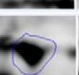
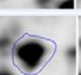
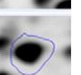
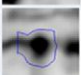
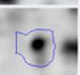
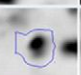
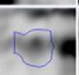
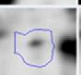
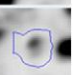
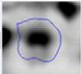
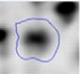
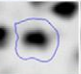
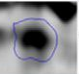
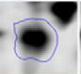
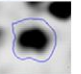



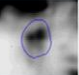
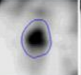
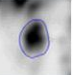
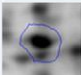
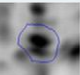
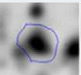
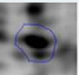
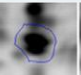
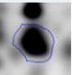
















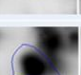

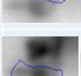





	Spot Number	Protein name	Control			Enrofloxacin		
1	179	biodegradative arginine decarboxylase						
2	447	alpha-galactosidase						
3	457	Tryptophanase						
4	561	6-phosphogluconate dehydrogenase, decarboxylating						
5	599	Sulfate adenylyltransferase subunit 1						
6	576	aspartate/ornithine carbamoyltransferase protein						
7	651	Transcriptional regulatory protein ZraR						
8	989	glucokinase						
9	963	Uridine phosphorylase						
10	999	Putative DNA-invertase from lambdoid prophage Qin						
11	1063	Flavoprotein WrbA						
12	1092	Outer membrane protein W						
13	1097	Superoxide dismutase [Fe]						
14	1108	Glucarate dehydratase						
15	1127	Glucose-specific phosphotransferase enzyme IIA component						
16	1157	ATP synthase subunit b						
17	1177	DNA protection during starvation protein						
18	1166	DNA protection during starvation protein						
19	1189	DNA protection during starvation protein						

Fig. 3. 2D DIGE details of the differentially expressed proteins with a p-value ≤ 0.05 and a fold change ≥ 2 .

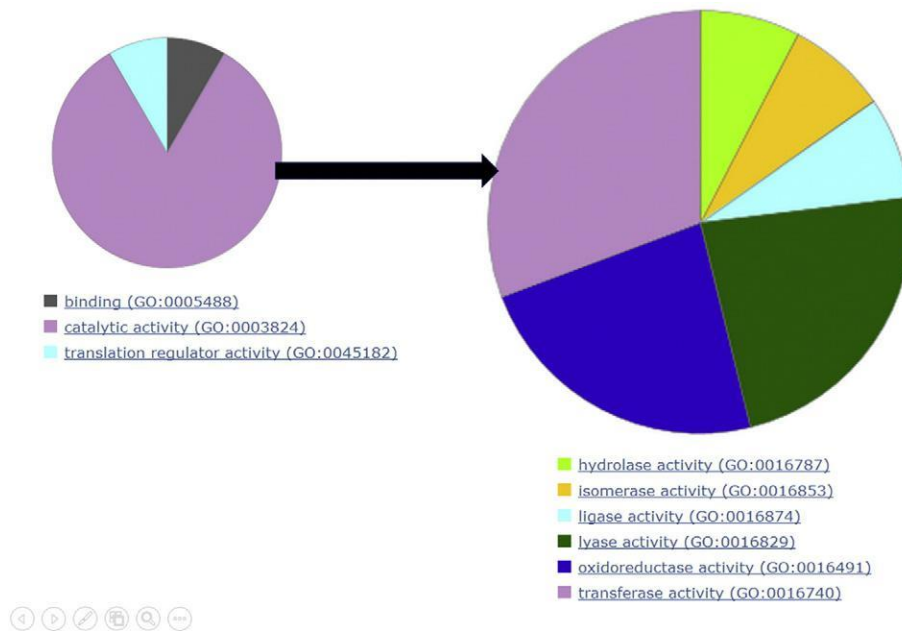


Fig. 4. Panther classification of 2D DIGE and shotgun MS differentially expressed proteins.

4.1. Metabolism

According to obtained data, energetic metabolism of *E. coli* resistant is generally depressed. This is logic because during the 'status' of antibiotic resistance bacteria try to survive and earn energy to fight against the an-tibiotics. The following proteins have been found to be differentially expressed.

4.1.1. ATP synthase subunit b (P0ABA0)

The link between defective ATP synthase and antibiotic resistance has been already described. In 1989 Humbert and Altendorf described a strain of *E. coli* cross-resistant to gentamicin, neomycin and streptomycin that was found to be defective for gamma subunit of ATP synthase (F1F0) [38]. A different result was found in *S. enterica* after quinolones exposure. ATP synthase, subunit b, was found to be increased after ciprofloxacin exposure [39]. As showed in Figs. 2, 3 and Table 1, obtained results highlight-ed a significantly decreased expression of ATP synthase, subunit b. This result may reflect the adaptive mechanism of the cell in the way of a silent mode in order to reduce the production of more oxidative stress. At the same time the *E. coli* cells are increasing the energy production from glycolysis. Another reason for the decreased expression of ATP synthase could be due to the different use of reducing power: in normal conditions reducing power can be used to generate the H⁺ gradient among the membrane in order to produce ATP, but, under oxidative stress conditions, such as enrofloxacin exposure, the reducing power is necessary to avoid oxidative-stress dependent DNA damage. As shown in Fig. 5, bioinformatic data analysis of obtained shotgun profiles confirmed the described evidence highlighting a decreasing amount of the bacterial subunits of ATP synthase.

4.1.2. Glucokinase (P0A6V8)

This is the first enzyme of glycolysis and is strongly down-regulated according to many of the enzymes of carbohydrate metabolism.

Shotgun MS analysis (Table 2) confirmed as well the previously de-scribed findings highlighting the down-regulation in the resistant group of proteins such as citrate synthase, succinate dehydrogenase, malate dehydrogenase and phosphoenolpyruvate synthase. This suggests that cells growing under enrofloxacin concentration present a decreased metabolism (Fig. 5).

4.1.3. Alpha galactosidase (P06720)

The down-regulation of α -galactosidase in resistant group is a new finding that emerged from obtained results. This result was firstly ob-served through 2D DIGE and successively confirmed by shotgun MS anal-ysis (Fig. 3, Table 1) that also highlighted a strong down-regulation in resistant isolates.

4.1.4. Glucose-specific phosphotransferase enzyme IIA component (P69783)

This protein is also involved in carbohydrates and sugar metabolism and is increased in resistant isolate as highlighted both by 2D DIGE ex-periments and shotgun MS analysis. It is part of the major carbohydrate transporter system and catalyzes the phosphorylation of incoming sugar substrates concomitantly with their translocation across the cell membrane. One of the GO terms (GO:0045912) associated with this protein is closely related to the negative regulation of carbohydrate metabolic process. Its up-regulation is in agreement with increased me-tabolism of carbohydrates in the resistant isolates in comparison with the control isolates.

Table 2

Differentially expressed proteins in two groups, enrofloxacin resistant (R) and control group (C), identified by label-free nUPLC-MS/MS.

Metabolism		Accession	Description	Score PLGS	Unique R:C	R:C Ratio	R:C Log(e) Ratio	R:C Log(e) StdDev
Metabolism	Metabolism, alpha-galactosidase activity	P06720	Alpha galactosidase	134.63	C			
	Metabolism, rotational mechanism	P0ABA0	ATP synthase subunit b	1167.56	C			
	Metabolism, glycolytic process	P0A6V8	Glucokinase	71.63	C			
	Metabolism, Tricarboxylic acid cycle	P0ABH8	Citrate synthase OS GN gltA	408.18	C			
	Metabolism, galactarate catabolic process	P0ABQ3	2 hydroxy 3 oxopropionate reductase	339.64	C			
	Metabolism, electron transport chain	P0AC43	Succinate dehydrogenase flavoprotein subunit GN sdhA	320.38	C			
	Metabolism, glycolytic process	P0AFG5	2 oxoglutarate dehydrogenase E1 component OS GN sucA	339.07	C			
	Metabolism, tricarboxylic acid cycle	P0AGF1	Succinyl CoA ligase ADP forming subunit alpha GN sucD	1265.07	C			
	Metabolism, gluconeogenesis	P23538	Phosphoenolpyruvate synthase GN ppsA PE 1 SV 5	145.73	C			
	Metabolism, malate metabolic process	P76251	D malate dehydrogenase decarboxylating GN dmlA	260.61	C			
	Metabolism, acetyl-CoA biosynthesis	P0A9M8	Phosphate acetyltransferase GN pta	171.09		0.59	-0.52	0.08
	Metabolism, pyruvate metabolic process	P06959	Dihydrolipoyllysine residue acetyltransferase component of pyruvate dehydrogenase complex	36.79		0.68	-0.38	0.09
	Metabolism, piruvate fermentation	P09373	Formate acetyltransferase 1 GN pflB	828.61		1.26	-0.23	0.03
	Metabolism acetyl-coA biosynthesis	P0A6A5	Acetate kinase OS GN ackA	511.32		0.70	-0.35	0.07
	Gluconeogenesis	A7ZUD3	Triosephosphate isomerase GN tpiA	828.39		1.69	0.52	0.06
Membrane transport	Cell outer membrane	P0A915	Outer membrane protein W	324.27	C			
	Sugar transport	P69783	Glucose-specific Phosphotransferase Enzyme IIA component	420.11	R			
	Cell outer membrane	P0A913	Peptidoglycan associated lipoprotein H7 GN pal	412.41	C			
	Cell outer membrane	P69778	Major outer membrane lipoprotein GN lpp	5434.85		0.27	-1.31	0.11
	Sugar transport	P69799	PTS system mannose specific EIIB component GN manX	283.55		0.59	-0.53	0.14
Protein metabolism	Pentose phosphate pathway	P00350	6 phosphogluconate dehydrogenase decarboxylating OS	74.47		1.63	0.49	0.02
	Glutamate degradation to GABA	Q8FHG5	Glutamate decarboxylase beta GN gadB	32.01	C			
	Proline metabolism	P09546	Bifunctional protein PutA GN putA	301.75	C			
	Amino-acid biosynthesis	A7ZR64	S adenosylmethionine synthase GN metK	171.62	R			
	Glutamate degradation to GABA	P58228	Glutamate decarboxylase alpha GN gadA	75.77		0.69	-0.37	0.05
	Protein biosynthesis	A7ZSL5	Elongation factor G GN fusA	668.20		0.70	-0.36	0.06
	Amino-acid biosynthesis	P0ABK6	Cysteine synthase A GN cysK	5377.78		4.76	1.56	0.19
	Aspartate metabolic process	Q8XDS0	Aspartate ammonia lyase GN aspA	2576.75		9.09	2.21	0.00
Translation process	Translation	A7ZSJ4	50S ribosomal protein L6 OS GN rplF	1122.51		0.32	-1.13	0.10
	Translation	P0AG69	30S ribosomal protein S1 GN rpsA	896.55		0.49	-0.71	0.05
	Translation	A7ZSJ5	30S ribosomal protein S4 GN rpsD	422.80		0.53	-0.63	0.08
	Translation	A7ZUJ6	50S ribosomal protein L11 GN rplK	1766.76		0.59	-0.52	0.04
	Translation	A7ZV74	50S ribosomal protein L9 GN rplI	4416.53		0.62	-0.48	0.03
	Translation	A7ZUJ8	50S ribosomal protein L10 GN rplJ	6836.01		0.63	-0.46	0.05
	Translation	A7ZSJ5	30S ribosomal protein S8 GN rpsH	2555.83		0.67	-0.39	0.10
	Translation	A7ZUJ7	50S ribosomal protein L1 GN rplA	2455.38		0.71	-0.34	0.05
	Translation	A7ZSK8	50S ribosomal protein L4 GN rplD	1946.56		0.76	-0.27	0.06
	Translation	B7UIL4	30S ribosomal protein S2 GN rpsB	1175.94		0.81	-0.21	0.07
	Translation	A7ZSL0	30S ribosomal protein S10 GN rpsJ	13.20		9.09	2.21	0.00
Oxidative stress response	Quinone oxidoreductase activity	P28304	Quinone oxidoreductase 1	138.32	R			
	Oxidation-reduction process	P0AGD3	Superoxide dismutase [Fe]	260.63	R			
	Stress response pathway	P14375	Transcriptional regulatory protein ZraR	413.25	R			
	Chaperone, protein folding	A7ZV11	10 kDa chaperonin GN groS PE 3 SV 1	3513.52		1.31	0.27	0.05
	Response to oxidative stress	P0AE10	Alkyl hydroperoxide reductase subunit C GN ahpC	3449.58		1.72	0.5	0.07
Cell-cell communication and quorum sensing	Protein folding	A7ZUJ4	Trigger factor GN tig	650.27	R			
	Tryptophan catabolism	P0A853	Tryptophanase OS	2407.49	C			
DNA repair	Pyrimidine biosynthesis	Q46803	Aspartate/ornithine carbamoyltransferase protein	69.80	C			
	Pyrimidine metabolism	P12758	Uridine phosphorylase	307.93		1.17	0.16	0.19
	DNA binding	P0ABT2	DNA protection during starvation protein dps	24296.61		3.45	1.24	0.05
	DNA binding	P77170	Putative DNA-invertase from lambdoid prophage Qin	48.52	C			
Other metabolisms	Arginine catabolic process	P28629	Biodegradative arginine decarboxylase	674.28	R			
	Sulfur compound metabolic process	P23845	Sulfate adenyltransferase subunit 1	61.18	C			
	D-glucarate catabolic process	P0AES2	Glucarate dehydratase	103.66	R			
	Nucleotide biosynthesis	A7ZIN4	Adenylate kinase OS GN adk	1650.37	R			
	Other	P64465	Putative selenoprotein YdfZ GN ydfZ	2310.80	R			

*Uniprot accession number.

4.2. Oxidative stress

Conversely, proteins that are responsible for activation of mechanism of reaction to oxidative stress are strongly over represented. In fact, it is well known that xenobiotics provoke a strong stress to bacterial cell, that is able to survive with more production of these proteins.

4.2.1. Phosphogluconate dehydrogenase (P00350)

This protein was found to be up-regulated with a 2,1 fold increase in resistant bacteria. It has been documented to be relevant to increase microbial resistance against oxidative compounds and its expression is activated in response to oxidative stress [40,41]. This demonstrates how this protein is important for cellular survival in presence of high concentration of oxidative compounds.

4.2.2. Quinone oxidoreductase 1 (P28304), flavoprotein WrbA (P0A8G6)

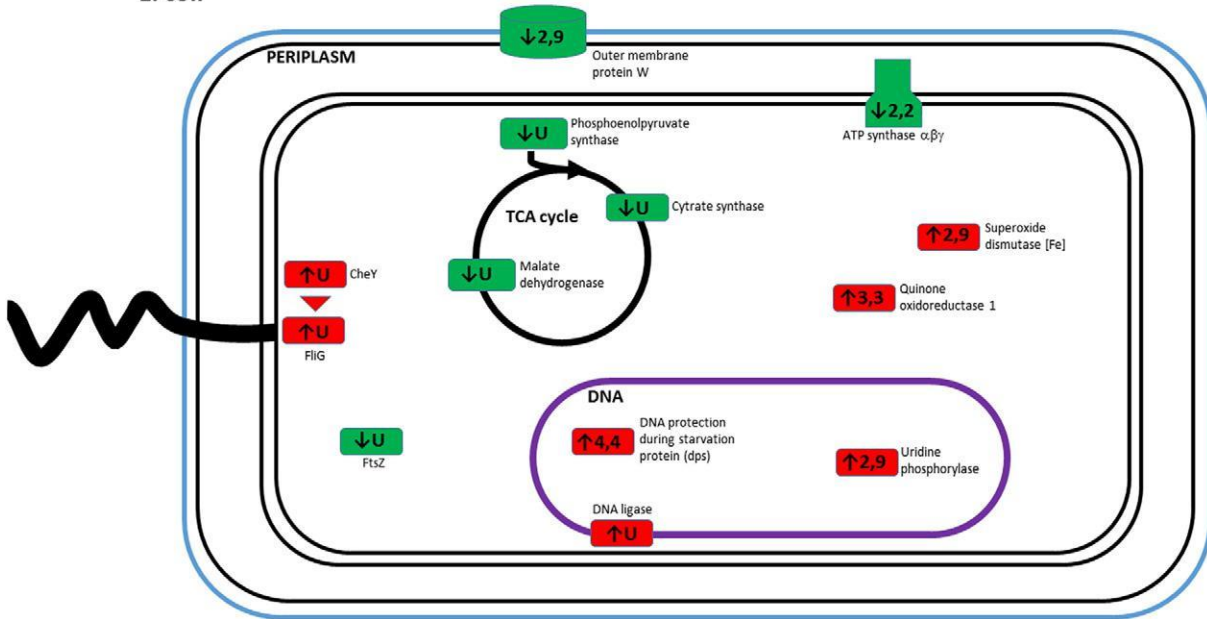
The flavoprotein WrbA has shown to have the enzymatic activity of a NADH (quinone oxidoreductase) suggesting its role in supply of reduced quinone and its relevance in counteract oxidative stress [42]. Many experimental evidences demonstrated that WrbA in *E. coli* is under the control of RpoS and, in turn, is positively regulated in response to an increased oxidative stress. But, more interesting, is the experimental evidence that documents how this protein is up-regulated in the early stage of stationary phase suggesting its putative role in preparing the cells for long-term survival under stress conditions, in this particular case, under subclinical antibiotic concentration [43–49].

4.2.3. Superoxide dismutase [Fe] (P0AGD3)

This protein showed a 2.9 fold increase confirmed by the same result in shotgun MS analysis. There are many evidences that document the role of this protein in the protection of *E. coli* cells from oxidative stress and xenobiotics more in general [50–52]. As well as its role in other species in increasing the resistance to antibiotics [52,53]. The relevance of this result confirms the key role played by the pathways involved in the counteraction of oxidative stress produced by xenobiotics and, in this case by enrofloxacin. Prevention of oxidative stress is also necessary for the protection of DNA that is particularly susceptible to damage due to the characteristics of this antibiotic. Bioinformatics analysis also confirmed the described result highlighting the expression of SOD only in the resistant isolate (Fig. 5).

Fig. 5. Overall scheme representing the key proteins involved in the mechanism of antibiotic resistance. In red the proteins up-regulated in E group (resistant) are represented and in green the proteins down-regulated. The values for each protein and the arrows indicate the trend and the fold change. In case of data from shotgun MS analysis, proteins unique of an experimental group have been labeled with U letter.

E. coli



4.2.4. Transcriptional regulatory protein ZraR (P14375)

This protein has found to be strongly up-regulated according to 2D DIGE and shotgun MS analysis. It is linked to the expression of ZraP protein that is positively regulated by the expression of ZraSR operon. ZraP protein, according to Corinne and colleagues [54], is a periplasmic molecular chaperon protein probably linked to the envelope stress response (ESR) pathways. Its up-regulation may be involved in the protection of this bacterium by noxious agents including a range of compounds with antimicrobial activity.

4.3. Membrane transport

4.3.1. Outer membrane protein W (P0A915)

Outer membrane proteins (OMPs) are located in outer bacterial membrane as permeability channels for nutrients, toxins, and antibiotics. It has been demonstrated that UPEC leads to an increase of secreted virulence factors and in particular of outer membrane associated proteins that cause alterations in the urinary tract [55–57]. For this reason recently the investigation of uropathogenic *E. coli* surface proteome is becoming a hot spot in order to find new diagnostic and therapeutic targets. Omps are involved in the host-pathogen interaction and are able to induce an immune response. *E. coli*. OmpA is involved in bacterial virulence and OmpC is involved in multidrug resistance. In particular it has been demonstrated that the absence of OmpC improves antibiotic resistance [58]. According to Hong and colleagues [59], the ompW forms an eight-stranded beta-barrel with a hydrophobic channel. As demonstrated by obtained results showed in Fig. 3 and resumed in Table 1, the expression of this protein decreased of 2.9 fold during enrofloxacin treatment according to 2D DIGE and this result was successively confirmed by shotgun MS analysis. This protein, according to the previously described experimental evidences, represents a channel through the outer membrane of this bacteria and its strong down-regulation during enrofloxacin treatment could suggest that it could represent one of the ways of entrance.

The decreased expression of this protein could limit the enrofloxacin passage and decrease its intracellular concentration.

4.4. Cell-cell communication and quorum sensing

4.4.1. Tryptophanase (P0A853)

This enzyme produces indole from tryptophan. Indole is a signaling molecule that is involved in regulation of several microbial processes as motility, biofilm formation and antibiotic resistance [60]. Its down-regulation in resistant group has been observed both in 2D DIGE experiments and in shotgun MS analysis.

4.4.2. Aspartate ammonia lyase (P0A853)

This enzyme is involved in the production of fumarate and ammonia (NH₃) volatile compound. It has been documented how this compound is able to modulate stress and drug response in physically separated bacteria [61]. Our results demonstrate that there is a strong down-regulation of this enzyme suggesting that this pathway is not stimulated or induced in this isolate by the administration of subclinical concentrations of this quinolone drug. This result in strong contrast with previous published papers that underline the involvement of this protein in the antibiotic resistance mechanisms [61,62]. However, a concordant result was published by Randall et al., demonstrating a strong downregulation of this protein in salmonella after disinfectant exposure [63].

About cell-cell communication, bioinformatic analysis highlighted the overexpression in resistant isolates of proteins such as CheZ (chemotaxis protein) and FliG (flagellar motor switch protein) as shown in Fig. 5. CheZ protein plays an important role in bacterial chemotaxis signal transduction pathway by accelerating the dephosphorylation of phosphorylated CheY (CheY-P). This protein is able to directly induce FliG and promote chemotaxis and cellular movement [64,65].

Quorum sensing mechanisms seem also to be activated in resistant cells according to the over-expression of proteins such as S adenosylmethionine synthase as reported in Table 2. S adenosylmethionine synthase is involved in the production of substrates involved in species-specific quorum sensing [66].

4.5. DNA repair

4.5.1. Aspartate/ornithine carbamoyltransferase protein (Q46803); aspartate carbamoyltransferase (Q46803)

This protein was found to be dramatically down-regulated in the resistant *coli*. This enzyme is typically described as involved in pyrimidine biosynthesis and, in turn, pyrimidine biosynthesis, represents one of the metabolic pathways that have been described to be inhibited by quinolones antibiotics in eukaryotes [67]. This finding could suggest that there is a negative regulation of pyrimidine biosynthesis in *E. coli* as in eukaryotes. To our knowledge, this is the first experimental evidence that documents the down-regulation of pyrimidine biosynthesis in *E. coli*. This was highlighted both by 2D DIGE experiments and successively validated through shotgun MS analysis and could suggest both an alternative mechanism of action of quinolones on prokaryotes or an adaptive mechanism analysis results. The reason of this differential expression is not fully understood but it was demonstrated in 1983 how in *E. coli* the acquired antibiotic resistance could increase the activity of uridine phosphorylase gene [70]. In our case, this evidence has been demonstrated at the protein expression level and in *E. coli* cells growing under subclinical concentration of enrofloxacin.

4.5.2. Uridine phosphorylase (P12758)

This protein catalyzes the synthesis of uridine to uracil [68,69]. As showed in results in Fig. 3 and Table 1 it is characterized by a differential expression of 2,9 fold in the resistant isolate confirmed by shotgun MS of *E. coli* to stop DNA synthesis in order to prevent supercoiling and DNA damage.

4.5.3. DNA protection during starvation protein (dps) (P0ABT2)

This is a protein of the stationary phase and it is able to bind the chromosome non-specifically in order to form a condensed form of dps-DNA condensed crystal structure that protects DNA from several sources of damage. It is also relevant in DNA protection from oxidative damage, UV radiation, metals toxicity and thermal shock [71–74]. As shown in Fig. 3 and Table 1, three isoforms of this protein were found to be up-regulated in the resistant isolate and the same trend was observed when analyzing the shotgun MS data. This strong protection of DNA is necessary to avoid DNA damage induced by enrofloxacin presence.

4.5.4. Putative DNA-invertase from lambdoid prophage Qin (P77170)

This protein has been found to be down-regulated in resistant isolates. According to uniprot database protein description it is involved in DNA integration and recombination. Its down-regulation looks apparently in contrast with the cell growth in enrofloxacin because of the need of *E. coli* cells for DNA rearrangements in order to promote mutations in the way of antibiotic resistance. But, according to the obtained data and to the quinolones function, its down-regulation could be due to a cellular strategy to keep DNA in this condition as stable as possible not promoting any DNA rearrangement.

As shown in 4, the resistant isolate showed the overexpression of DNA ligase that is a protein strongly involved in bases excision and DNA repair process.

4.6. Other metabolisms

4.6.1. Biodegradative arginine decarboxylase (P28629)

It has been documented [75] how arginine decarboxylase synthesis is dependent to *cysB* regulator which, in turn, is linked to an increased antibiotic resistance in *E. coli* in the swarm state. Obtained results highlighted a 2 fold increased expression of this protein in resistant *E. coli*, suggesting an increased regulation of this operon or, at least, an potential involvement of this protein in the development of antibiotic resistance.

4.6.2. Sulfate adenylyltransferase subunit 2 (P23845)

It is a protein involved in sulfur metabolism. It showed a down-regulation of 2.6 suggesting a putative decrease of this pathway in the resistant isolate.

4.6.3. Glucarate dehydratase (P0AES2)

This protein was found to be strongly up-regulated in resistant in comparison to sensitive isolate. This result was firstly found by 2D electro-phoresis and then confirmed by shotgun MS. The function of this protein seems to be linked to the amino acid catabolic process but its role in quinolones resistance and the reason for its up-regulation is still object of study.

4.6.4. Trigger factor GN (A7ZIJ4)

It was found to be upregulated in enrofloxacin (Table 2) resistant isolates and it has been found to have a function as chaperon protein [76].

5. Conclusion

The applied complementary approach described allowed the identification of key proteins and pathways involved in the development of antibiotic resistance due to *E. coli* growth in presence of enrofloxacin. Bioinformatics analysis, as showed in Fig. 5, demonstrates how the proteins involved in cell replication process are more expressed in the control isolates. These proteins are involved in cell division process as (FtsZ), replicative DNA helicase and ATP-dependent Lon protease. All these proteins are also involved in the enhancement of cell replication and growth and are only expressed in the control isolates. Quinone ox-reductase 1 is characteristic of the stationary phase and a key protein in preparing the cells to long-term survival under stress conditions. As well as Dps protein is a typical protein of stationary phase involved in the stabilization of double strand DNA filament in order to prevent oxidative-stress-dependent damage. Our results also showed that resistant cells enhance several pathways involved in the response to oxidative stress and in turn to the production of reducing power.

The drastic down-regulation of OmpW, which represents one of the main gates for enrofloxacin entrance, could be an additional mechanism of *E. coli* defense against enrofloxacin. In fact reducing intracellular concentration of enrofloxacin and, more in general, of putative toxic compounds or xenobiotics, represents one of the most effective ways to improve survival in hostile environments.

All these mechanisms are the cause of an increased antibiotic resistance and could represent putative targets for the development of new ways to counteract drug and multidrug resistance. This represents a key point, specially if considering that the new reservoirs of these resistant zoonotic agents could be pets.

Moreover, it remains to be elucidated if the mechanisms involved in drug resistance in dog *E. coli* isolates are the same of human *E. coli* isolates. If the human isolates exposed to the same concentration of enrofloxacin show the same adaptive mechanisms it can be hypothesized that the pathways involved in this phenomenon are similar.

Supplementary data to this article can be found online at <http://dx.doi.org/10.1016/j.jprot.2015.05.040>.

Acknowledgments and funding

Authors are grateful to the COST action 1002 FAP for the network provided and to the project "Piano di Sviluppo - UNIMI" (to A.S.) for the support.

References

- [1] X. Zhang, et al., Prevalence of veterinary antibiotics and antibiotic-resistant *Escherichia coli* in the surface water of a livestock production region in northern China, *PLoS One* 9 (11) (2014) e111026.
- [2] M.-T. Labro, J.-M. Bryskier, Antibacterial resistance: an emerging zoonosis? *Expert Rev. Anti-Infect. Ther.* 12 (12) (2014) 1441–1461.
- [3] G. Cheng, et al., Antibiotic alternatives: the substitution of antibiotics in animal husbandry? *Front. Microbiol.* (2014) 5.
- [4] V. Viswanathan, Off-label abuse of antibiotics by bacteria, *Gut Microbes* 5 (1) (2014) 3–4.
- [5] L. Clemente, et al., Occurrence of extended-spectrum β -lactamases among isolates of *Salmonella enterica* subsp. *enterica* from food-producing animals and food products, in Portugal, *Int. J. Food Microbiol.* 167 (2) (2013) 221–228.
- [6] C. Piras, et al., Comparative proteomics to evaluate multi drug resistance in *Escherichia coli*, *Mol. BioSyst.* 8 (4) (2012) 1060–1067.
- [7] I. Jorgensen, P.C. Seed, How to make it in the urinary tract: a tutorial by *Escherichia coli*, *PLoS Pathog.* 8 (10) (2012) e1002907.
- [8] B. Foxman, Epidemiology of urinary tract infections: incidence, morbidity, and economic costs, *Am. J. Med.* 113 (1) (2002) 5–13.
- [9] L. Jakobsen, et al., Is *Escherichia coli* urinary tract infection a zoonosis? Proof of direct link with production animals and meat, *Eur. J. Clin. Microbiol. Infect. Dis.* 31 (6) (2012) 1121–1129.
- [10] J.R. Johnson, et al., Antimicrobial drug-resistant *Escherichia coli* from humans and poultry products, Minnesota and Wisconsin, 2002–2004, *Emerg. Infect. Dis.* 13 (6) (2007) 838.
- [11] J.R. Johnson, et al., Identification of urovirulence traits in *Escherichia coli* by comparison of urinary and rectal *E. coli* isolates from dogs with urinary tract infection, *J. Clin. Microbiol.* 41 (1) (2003) 337–345.
- [12] S.-K. Chang, et al., Antimicrobial resistance of *Escherichia coli* isolates from canine urinary tract infections, *J. Vet. Med. Sci.* 77 (1) (2015) 59–65.
- [13] J.R. Johnson, et al., Evidence of commonality between canine and human extraintestinal pathogenic *Escherichia coli* strains that express *papG* allele III, *Infect. Immun.* 68 (6) (2000) 3327–3336.
- [14] J.R. Johnson, A.L. Stell, P. Delavari, Canine feces as a reservoir of extraintestinal pathogenic *Escherichia coli*, *Infect. Immun.* 69 (3) (2001) 1306–1314.
- [15] S.A. Aly, et al., Molecular mechanisms of antimicrobial resistance in fecal *Escherichia coli* of healthy dogs after enrofloxacin or amoxicillin administration, *Can. J. Microbiol.* 58 (11) (2012) 1288–1294.
- [16] C.L. Cooke, et al., Enrofloxacin resistance in *Escherichia coli* isolated from dogs with urinary tract infections, *J. Am. Vet. Med. Assoc.* 220 (2) (2002) 190–192.
- [17] C. Levine, H. Hiasa, K.J. Marians, DNA gyrase and topoisomerase IV: biochemical activities, physiological roles during chromosome replication, and drug sensitivities, *Biochim. Biophys. Acta Gene Struct. Expr.* 1400 (1) (1998) 29–43.
- [18] K. Drlica, Mechanism of fluoroquinolone action, *Curr. Opin. Microbiol.* 2 (5) (1999) 504–508.
- [19] M. del Mar Tavio, et al., Mechanisms involved in the development of resistance to fluoroquinolones in *Escherichia coli* isolates, *J. Antimicrob. Chemother.* 44 (6) (1999) 735–742.
- [20] M. Karczmarczyk, et al., Mechanisms of fluoroquinolone resistance in *Escherichia coli* isolates from food-producing animals, *Appl. Environ. Microbiol.* 77 (20) (2011) 7113–7120.
- [21] L. Putignani, et al., MALDI-TOF mass spectrometry proteomic phenotyping of clinically relevant fungi, *Mol. BioSyst.* 7 (3) (2011) 620–629.
- [22] C. Piras, et al., Identification of immunoreactive proteins of *Mycobacterium avium* subsp. *paratuberculosis*, *Proteomics* 15 (4) (2015) 813–823.
- [23] A. Shevchenko, et al., In-gel digestion for mass spectrometric characterization of proteins and proteomes, *Nat. Protoc.* 1 (6) (2006) 2856–2860.
- [24] A. Shevchenko, et al., Mass spectrometric sequencing of proteins from silver-stained polyacrylamide gels, *Anal. Chem.* 68 (5) (1996) 850–858.
- [25] M. De Canio, et al., Differential protein profile in sexed bovine semen: shotgun proteomics investigation, *Mol. BioSyst.* 10 (6) (2014) 1264–1271.
- [26] A. Soggiu, et al., Unravelling the bull fertility proteome, *Mol. BioSyst.* 9 (6) (2013) 1188–1195.
- [27] J.C. Silva, et al., Absolute quantification of proteins by LCMSE: a virtue of parallel MS acquisition, *Mol. Cell. Proteomics* 5 (1) (2006) 144–156.
- [28] J.P. Vissers, J.I. Langridge, J.M. Aerts, Analysis and quantification of diagnostic serum markers and protein signatures for Gaucher disease, *Mol. Cell. Proteomics* 6 (5) (2007) 755–766.
- [29] J.A. Vizcaino, et al., The Proteomics IDENTifications (PRIDE) database and associated tools: status in 2013, *Nucleic Acids Res.* 41 (D1) (2013) D1063–D1069.
- [30] J.A. Vizcaino, et al., ProteomeXchange provides globally coordinated proteomics data submission and dissemination, *Nat. Biotechnol.* 32 (3) (2014) 223–226.
- [31] P. Jones, et al., InterProScan 5: genome-scale protein function classification, *Bioinform. Methods* 30 (9) (2014) 1236–1240.
- [32] H. Mi, et al., Large-scale gene function analysis with the PANTHER classification system, *Nat. Protoc.* 8 (8) (2013) 1551–1566.
- [33] C. Camacho, et al., BLAST+: architecture and applications, *BMC Bioinformatics* 10 (2009) 421.
- [34] D.H. Huson, N. Weber, Microbial community analysis using MEGAN, *Methods Enzymol.* 531 (2013) 465–485.
- [35] A. Borovskaya, et al., Differentiation of α -hemolytic streptococci by direct mass spectrometric profiling, *Russ. J. Bioorg. Chem.* 37 (1) (2011) 53–60.
- [36] W. AndjãTao, Rapid ambient mass spectrometric profiling of intact, untreated bacteria using desorption electrospray ionization, *Chem. Commun.* 1 (2007) 61–63.
- [37] M. Kostrzewa, et al., MALDI-TOF MS: an upcoming tool for rapid detection of antibiotic resistance in microorganisms, *Proteomics Clin. Appl.* 7 (11–12) (2013) 767–778.
- [38] R. Humbert, K. Altendorf, Defective gamma subunit of ATP synthase (F1F0) from *Escherichia coli* leads to resistance to aminoglycoside antibiotics, *J. Bacteriol.* 171 (3) (1989) 1435–1444.
- [39] N.G. Coldham, et al., Effect of fluoroquinolone exposure on the proteome of *Salmonella enterica* serovar Typhimurium, *J. Antimicrob. Chemother.* 58 (6) (2006) 1145–1153.
- [40] B.E. Lundberg, et al., Glucose 6-phosphate dehydrogenase is required for *Salmonella typhimurium* virulence and resistance to reactive oxygen and nitrogen intermediates, *Infect. Immun.* 67 (1) (1999) 436–438.
- [41] W.P. Fawcett, R. Wolf, Genetic definition of the *Escherichia coli* *zwf* "soxbox," the DNA binding site for SoxS-mediated induction of glucose 6-phosphate dehydrogenase in response to superoxide, *J. Bacteriol.* 177 (7) (1995) 1742–1750.
- [42] S.L. Andrade, et al., Crystal structure of the NADH: quinone oxidoreductase WrbA from *Escherichia coli*, *J. Bacteriol.* 189 (24) (2007) 9101–9107.
- [43] D.E. Chang, D.J. Smalley, T. Conway, Gene expression profiling of *Escherichia coli* growth transitions: an expanded stringent response model, *Mol. Microbiol.* 45 (2) (2002) 289–306.
- [44] K.J. Cheung, et al., A microarray-based antibiotic screen identifies a regulatory role for supercoiling in the osmotic stress response of *Escherichia coli*, *Genome Res.* 13 (2) (2003) 206–215.
- [45] K.A. Jensen Jr., et al., An NADH: quinone oxidoreductase active during biodegradation by the brown-rot basidiomycete *Gloeophyllum trabeum*, *Appl. Environ. Microbiol.* 68 (6) (2002) 2699–2703.
- [46] S. Phadtare, I. Kato, M. Inouye, DNA microarray analysis of the expression profile of *Escherichia coli* in response to treatment with 4, 5-dihydroxy-2-cyclopenten-1-one, *J. Bacteriol.* 184 (23) (2002) 6725–6729.
- [47] P.J. Pomposiello, M.H. Bennik, B. Dimple, Genome-wide transcriptional profiling of the *Escherichia coli* responses to superoxide stress and sodium salicylate, *J. Bacteriol.* 183 (13) (2001) 3890–3902.
- [48] D.L. Tucker, N. Tucker, T. Conway, Gene expression profiling of the pH response in *Escherichia coli*, *J. Bacteriol.* 184 (23) (2002) 6551–6558.
- [49] E.V. Patridge, J.G. Ferry, WrbA from *Escherichia coli* and *Archaeoglobus fulgidus* is an NAD(P)H: quinone oxidoreductase, *J. Bacteriol.* 188 (10) (2006) 3498–3506.
- [50] C. Geslin, et al., The manganese and iron superoxide dismutases protect *Escherichia coli* from heavy metal toxicity, *Res. Microbiol.* 152 (10) (2001) 901–905.
- [51] M.Y. Gruber, B.R. Glick, J.E. Thompson, Cloned manganese superoxide dismutase reduces oxidative stress in *Escherichia coli* and *Anacystis nidulans*, *Proc. Natl. Acad. Sci.* 87 (7) (1990) 2608–2612.
- [52] J.T. Greenberg, et al., Positive control of a global antioxidant defense regulon activated by superoxide-generating agents in *Escherichia coli*, *Proc. Natl. Acad. Sci.* 87 (16) (1990) 6181–6185.
- [53] F.B. Nogueira, et al., Increased expression of iron-containing superoxide dismutase-A (TcFeSOD-A) enzyme in *B. i. N. Trypanosoma cruzi* *B. i. N.* population with *B. i. N.* in vitro *B. i. N.*-induced resistance to benzimidazole, *Acta Trop.* 100 (1) (2006) 119–132.
- [54] A.-A. Corinne, et al., ZraP is a periplasmic molecular chaperone and a repressor of the zinc-responsive two-component regulator ZraSR, *Biochem. J.* 442 (1) (2012) 85–93.
- [55] D.J. Worpel, et al., Comparative analysis of the uropathogenic *Escherichia coli* surface proteome by tandem mass-spectrometry of artificially induced outer membrane vesicles, *J. Proteomics* 115 (2015) 93–106.
- [56] F.B. Scorza, et al., Proteomics characterization of outer membrane vesicles from the extraintestinal pathogenic *Escherichia coli* tolR IHE3034 mutant, *Mol. Cell. Proteomics* 7 (3) (2008) 473–485.
- [57] M. Totsika, et al., Uropathogenic *Escherichia coli* mediated urinary tract infection, *Curr. Drug Targets* 13 (11) (2012) 1386–1399.
- [58] Y.-F. Liu, et al., Loss of outer membrane protein C in *Escherichia coli* contributes to both antibiotic resistance and escaping antibody-dependent bactericidal activity, *Infect. Immun.* 80 (5) (2012) 1815–1822.
- [59] H. Hong, et al., The outer membrane protein OmpW forms an eight-stranded β -barrel with a hydrophobic channel, *J. Biol. Chem.* 281 (11) (2006) 7568–7577.
- [60] G. Li, K.D. Young, Indole production by the tryptophanase TnaA in *Escherichia coli* is determined by the amount of exogenous tryptophan, *Microbiology* 159 (Pt 2) (2013) 402–410.
- [61] S.P. Bernier, et al., Biogenic ammonia modifies antibiotic resistance at a distance in physically separated bacteria, *Mol. Microbiol.* 81 (3) (2011) 705–716.
- [62] S. Maria-Neto, et al., Deciphering the magainin resistance process of *Escherichia coli* strains in light of the cytosolic proteome, *Antimicrob. Agents Chemother.* 56 (4) (2012) 1714–1724.
- [63] L. Randall, et al., Commonly used farm disinfectants can select for mutant *Salmonella enterica* serovar Typhimurium with decreased susceptibility to biocides and antibiotics without compromising virulence, *J. Antimicrob. Chemother.* 60 (6) (2007) 1273–1280.

- [64] H. Wang, P. Matsumura, Characterization of the CheAS/CheZ complex: a specific interaction resulting in enhanced dephosphorylating activity on CheY-phosphate, *Mol. Microbiol.* 19 (4) (1996) 695–703.
- [65] K.C. Boesch, R.E. Silversmith, R.B. Bourret, Isolation and characterization of nonchemotactic CheZ mutants of *Escherichia coli*, *J. Bacteriol.* 182 (12) (2000) 3544–3552.
- [66] S.P. Zano, et al., Alternative substrates selective for S-adenosylmethionine synthetases from pathogenic bacteria, *Arch. Biochem. Biophys.* 536 (1) (2013) 64–71.
- [67] A. Forsgren, et al., Effects of ciprofloxacin on eucaryotic pyrimidine nucleotide biosynthesis and cell growth, *Antimicrob. Agents Chemother.* 31 (5) (1987) 774–779.
- [68] I. Oliva, et al., Characterization of *Escherichia coli* uridine phosphorylase by single-site mutagenesis, *J. Biochem.* 135 (4) (2004) 495–499.
- [69] T.T. Caradoc-Davies, et al., Crystal structures of b i N *Escherichia coli* b/i N uridine phosphorylase in Two native and three complexed forms reveal basis of substrate specificity, induced conformational changes and influence of potassium, *J. Mol. Biol.* 337 (2) (2004) 337–354.
- [70] M. Astvatsaturian, A. Mironov, V. Sukhodolets, Mutations of resistance to rifampicin leading to increased activity of the uridine phosphorylase gene in *Escherichia coli*, *Genetika* 19 (7) (1983) 1070.
- [71] M. Almiron, et al., A novel DNA-binding protein with regulatory and protective roles in starved *Escherichia coli*, *Genes Dev.* 6 (12b) (1992) 2646–2654.
- [72] S.G. Wolf, et al., DNA protection by stress-induced biocrystallization, *Nature* 400 (6739) (1999) 83–85.
- [73] S. Nair, S.E. Finkel, Dps protects cells against multiple stresses during stationary phase, *J. Bacteriol.* 186 (13) (2004) 4192–4198.
- [74] P. Ceci, et al., DNA condensation and self-aggregation of *Escherichia coli* Dps are coupled phenomena related to the properties of the N-terminus, *Nucleic Acids Res.* 32 (19) (2004) 5935–5944.
- [75] A.L. Turnbull, M.G. Surette, L-Cysteine is required for induced antibiotic resistance in actively swarming *Salmonella enterica* serovar Typhimurium, *Microbiology* 154 (11) (2008) 3410–3419.
- [76] G. Kramer, et al., L23 protein functions as a chaperone docking site on the ribosome, *Nature* 419 (6903) (2002) 171–174.